NUMERICAL SIMULATION OF JANUARY 28 COLD AIR OUTBREAK DURING *GALE* PART I: THE MODEL AND SENSITIVITY TESTS OF TURBULENCE CLOSURES

CHING-YUANG HUANG and SETHU RAMAN

Department of Marine, Earth and Atmospheric Sciences, North Carolina State University, Raleigh, NC, 27695-8208, U.S.A.

(Received in final form 9 January, 1991)

Abstract. A mesoscale planetary boundary layer (PBL) numerical model has been developed to study airflow over complex topography. Turbulence closures using the turbulent kinetic energy (TKE) and dissipation (ϵ) equations are investigated in combination with the level 2.5 scheme of Mellor and Yamada (1982) to determine eddy diffusivities for momentum and heat. This modified E-ϵ closure is simpler than the level 3 one which requires more prognostic equations for moist turbulent transport.

One-dimensional (1-D) model results show that the PBL mean flows under various stability conditions are not significantly sensitive to the modified Blackadar and Kolmogorov eddy mixing-length formulations used in this E-ϵ model, although the latter yields excessively large mixing lengths in the entrainment region of the upper PBL. Eddy mixing lengths in the Kolmogorov-type formulation can be better defined by introducing background dissipation. Using the same prognostic TKE equation, the 1-D model results are not significantly affected by different diagnostic formulations in the closures. The simulated results compare well with large-eddy simulations and those obtained using higher-order closure schemes including the level 3 one. The results are found to be insensitive to eddy Prandtl number, in contrast to the 2-D model results (see Part II).

1. Introduction

Cold air outbreak is a strong synoptic event over the Atlantic Ocean off the U.S. southeast coast during winters. One such event was observed during the Intensive Observation Period-2 (IOP-2) of the Genesis of Atlantic Lows Experiment (GALE) in 1986 (see Dirks *et al.*, 1988). Boundary-layer modification occurs as the cold air moves over the warmer ocean and the Gulf Stream with a sea surface temperature (SST) of about 25°C, causing strong surface heat fluxes (Wayland and Raman, 1989). In addition to the effects of surface warming, the atmospheric baroclinicity induced by strong horizontal temperature gradients may lead to the development of Gulf Stream cloud/rain bands (Huang and Raman, 1990a).

The strong interaction of the airflow and the Gulf Stream baroclinic zone is important for the offshore development of cyclones since the upward heat flux from the ocean could supply sufficient energies into the system. Cyclones tend to become explosive as the embedded cold front passes over the Gulf Stream baroclinic zone. A coastal front and an offshore cyclogenesis occurred during the GALE IOP-2. As the cold front associated with such a cyclone moves offshore, a convective marine boundary layer (MBL) develops and slopes seaward. The

Boundary-Layer Meteorology **55**: 381–407, 1991.

MBL resembles a convective boundary layer (CBL) over land, but the observed turbulent heat fluxes in the former case can be one order larger and possibly condition the atmosphere for a quicker development of the cyclone.

In order to model the variation of the MBL over this region, one must rely on turbulence parameterizations. Since computer power has increased greatly in recent years, use of a high-order turbulence closure in mesoscale models is no longer prohibitive. Turbulence closures may extend to even third order (e.g., André *et al.*, 1978), which involve several tens of prognostic equations for turbulent moments in addition to those for mean flow. Third-order closures are very time-consuming in computation and are quite complicated particularly when applied to multi-dimensional simulations.

A complete version of the second-order closure (Mellor and Yamada, 1982), the level 4, requires about twenty prognostic equations, and a simplified version, the level 3, at least 4 for moist flow. Both the level 4 (or similar complex schemes) and level 3 have been incorporated into 2-D models (see Mellor and Yamada, 1982). As shown in Yamada and Mellor (1975), the level 4 and level 3 predict 1-D CBL flow in a similar manner. Partial effects of counter-gradient transport could also be retained in the level 3 (e.g., Sun and Ogura, 1980). A simplified version of the level 3 is the level 2.5. At this level, all the turbulence covariances are neglected, leaving only the prognostic turbulent kinetic energy (TKE) equation. Although the level 2.5 neglects all covariances, it behaves in an approximately similar manner as the level 3 (Mellor and Yamada, 1982).

A significant assumption in the M-Y (Mellor-Yamada) type of second-order closures is the use of Kolmogorov's hypothesis for diagnosing turbulent dissipation (ϵ). An alternative would be to employ an additional prognostic ϵ-equation (e.g., Duynkerke and Driedonks, 1987; Duynkerke, 1988; Holt and Raman, 1988; Holt *et al.*, 1990). Since turbulent dissipation is prognostic in the E-ϵ closure, it can be used to parameterize eddy mixing length, in contrast to the Blackadar-type of formulation which depends on some presumed length scales.

One of the benefits in the level 2.5 is that eddy Prandtl number is not assumed. The level 2.5 has been used in a number of numerical models including general circulation models (see Mellor and Yamada, 1982). The E-ϵ closure, despite the simple assumption for eddy Prandtl number, is capable of obtaining characteristic boundary-layer structures (e.g., Huang and Raman, 1989; Holt *et al.*, 1990). Both closures (level 2.5 and E-ϵ) are appropriate for use in 3-D simulations because of computational efficiency.

Objectives of Part I are to investigate the possibility of combining the beneficial features of the level 2.5 and the E-ϵ closure, to study the role of eddy Prandtl number in changing the behaviors of the turbulence, and to examine the reliability of closure schemes with different eddy mixing-length parameterizations. The suitability of a specific eddy mixing formulation may be easily understood in terms of the 1-D model results. On the basis of the 1-D model results, comparisons of turbulence parameterizations are extended to 2-D flow. In Part II, the January 28

cold air outbreak over the Gulf Stream region is simulated, and the model results are compared with the observations (Wayland and Raman, 1989).

2. The Numerical Model

The present model is a modified version of those of Huang and Raman (1989; 1990a). In the present model, liquid water has been partitioned into cloud water and rain water. The hydrostatic and anelastic approximations are still assumed. The model is 3-D, but it also allows 2-D simulation. Its 3-D formulations of the governing equations and cloud microphysics are described in detail by Huang (1990).

2.1. Turbulence closures

The atmospheric PBL is treated as the surface layer (SL) and the transition layer, separately. The surface-layer turbulent transport obeys the similarity stability functions given by Businger *et al.* (1971). Above the surface layer, the prognostic TKE and turbulent dissipation equations are used. Details of the turbulence closures are provided in the Appendix of this paper.

2.2. Numerical aspects

A detailed description of the numerical aspects including the boundary conditions is given by Huang (1990). The numerical scheme used for horizontal advection is a two-time-level fourth-order Crowley scheme (Huang and Raman, 1990b), which is based on the multi-step WKL scheme (Warming *et al.*, 1973). The new scheme, termed the modified WKL scheme, uses a free parameter to minimize numerical dispersion and dissipation, and thus is very reliable in representing the advection of positive-definite scalars such as moisture, TKE and turbulent dissipation. The scheme has been shown to be comparable to the fourth-order leapfrog scheme and the cubic upstream spline (Huang and Raman, 1990b). For vertical advection, the quadratic upstream interpolation is adopted since the scheme requires one grid less than the modified WKL scheme. The two advection schemes are at least third order accurate; their formulations can be found in Huang (1990) and Huang and Raman (1990b).

3. The 1-D Model Results

A one-dimensional PBL model is used to investigate various closure assumptions in the E-model, the E-ϵ model and the E-ϵ model combined with the level 2.5 one (for details of the turbulence closures see Appendix). Table I describes the model parameters and some results for three different types of PBLs, i.e., neutral PBL (denoted as case R1), diurnal PBL (R2) and convective MBL (R3). The 1-D flow is governed by the set of Ekman-gradient wind equations (see Huang and Raman, 1988). Advection effects are not prescribed. Since these numerical

TABLE I

Numerical experiments and salient model results for different 1-D PBL closure schemes. The inverse Prandtl number P_{rt} is defined as K_θ/K_M. For the definitions of the modified Blackadar (denoted as BL) and Kolmogorov (denoted as KL) mixing-length formulations, see the text.

α, β	zf/u_* for max. K_M	Max. $K_M f/u_*^2$	Max. P_{rt}	Mixing length formulation	Closure model
R1 (neutral PBL), $z_0 = 0.018\, u_*^2/g$					
$\alpha = 0.05$	0.254	0.026	1.25	*BL*	*E-ϵ*
$\alpha = 0.1$	0.357	0.040	1.27	*BL*	E-ϵ
$\alpha = 0.2$	0.488	0.060	1.50	*BL*	E-ϵ
$\beta = 2$	0.351	0.031	1.23	*KL*	E-ϵ
$\beta = 4$	0.463	0.041	1.23	*KL*	E-ϵ
$\beta = \infty$	0.760	0.079	1.23	*KL*	E-ϵ
R2 (diurnal PBL), $z_0 = 1\ cm$					
$\alpha = 0.1$			1.37	*BL*	*E-ϵ*
$\beta = \infty$				*KL*	E-ϵ
$\alpha = 0.1$			1.0	*BL*	E

α, β, c_w	Hour	u_* (m s^{-1})	w_* (m s^{-1})	E_{max}/E_{sfc}	Max. K_M (m^2 s^{-1})	PBL height (m)
R3 (convective MBL), $z_0 = 0.018\, u_*^2/g$						
$\alpha = 0.1$,	6	0.48	2.85	1.59	206 at 850 m	2300
$c_w = 0.2$	12	0.51	2.96	1.61	293 at 1150 m	3100
$\alpha = 0.01$,	6	0.48	2.85	3.01	208 at 850 m	2250
$c_w = 0.0$	12	0.51	2.85	2.94	294 at 1150 m	3000
$\alpha = 0.05$,	6	0.46	2.68	3.90	90 at 700 m	2000
$c_w = 0.0$	12	0.49	2.81	3.96	135 at 1000 m	2850

experiments are intended only as sensitivity tests, moisture effects (including condensation) are neglected to keep the 1-D model simple. Case R1 simulates a neutral boundary-layer flow over the ocean. The results for this simple case (R1) can be compared with those using higher-order closures and LES models. All three cases assume a constant geostrophic wind of $U_g = V_g = 10$ m s^{-1} within the whole model domain containing 81 grids with a uniform interval of 50 m. Since turbulent transfer is computed using a time-implicit scheme, a large time step Δt of 120 s can be chosen (for time-explicit schemes, it drops below 5 s). At the upper boundary, second-order derivatives of TKE and turbulent dissipation and first-order derivatives of wind components vanish for R2 and R3, while the potential temperature is kept unchanged. For R1, TKE and turbulent dissipation are assumed to vanish at the upper boundary.

3.1. Neutral PBL

Figures 1 and 2 show the variations of normalized l and K_M with the nondimensional height, $zf/u*$ for near steady-state conditions for the modified Blackadar

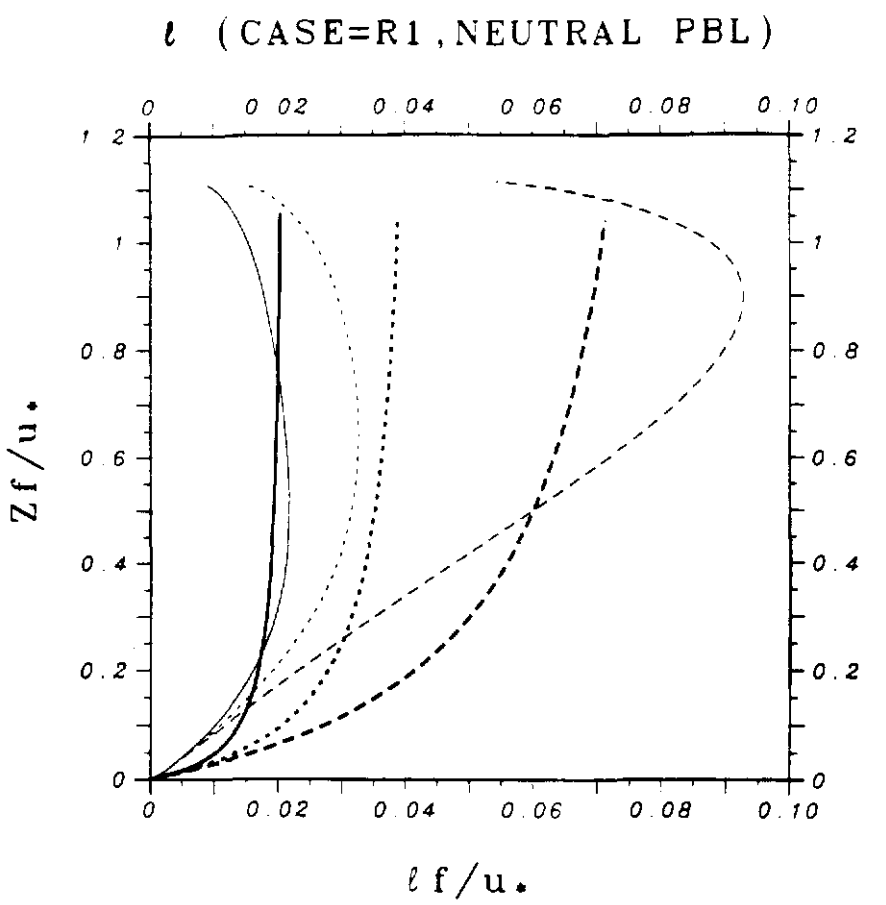

Fig. 1. Variation of the normalized mixing length ($l\,f/u_*$) at steady state for different PBL closures used in a neutral boundary layer (see Table I). Bold lines are for the modified Blackadar mixing-length formulation with $\alpha = 0.05$ (solid line), $\alpha = 0.1$ (shorter dashed) and $\alpha = 0.2$ (longer dashed); thin lines for Kolmogorov's formulation with $\beta = 2$ (solid), $\beta = 4$ (shorter dashed) and $\beta = \infty$ (longer dashed).

eddy mixing length formulation (bold lines) and Kolmogorov formulation (thin lines) (hereafter referred to as BL and KL, respectively). Details of both formulations are given in Appendix. As can be seen in Figure 1, the BL run shows monotonically increasing mixing length with height, while the KL run using $\beta = \infty$ (long-dashed lines) shows a mixing length that decreases with height at the upper levels of the neutral boundary layer. The mixing length at lower levels increases linearly with height as normally found in the E-ϵ model with KL formulation (see Duynkerke, 1988). It appears that the E-ϵ model using KL is more sensitive to the upper boundary conditions than the one using BL. With the modified KL which introduces background dissipation (see Appendix), the E-ϵ model provides more reasonable eddy mixing lengths at upper levels. In Figure 2 for normalized K_M profiles, BL and KL give results similar to those in Figure 1, except that K_M decays to zero because of the imposed upper boundary conditions.

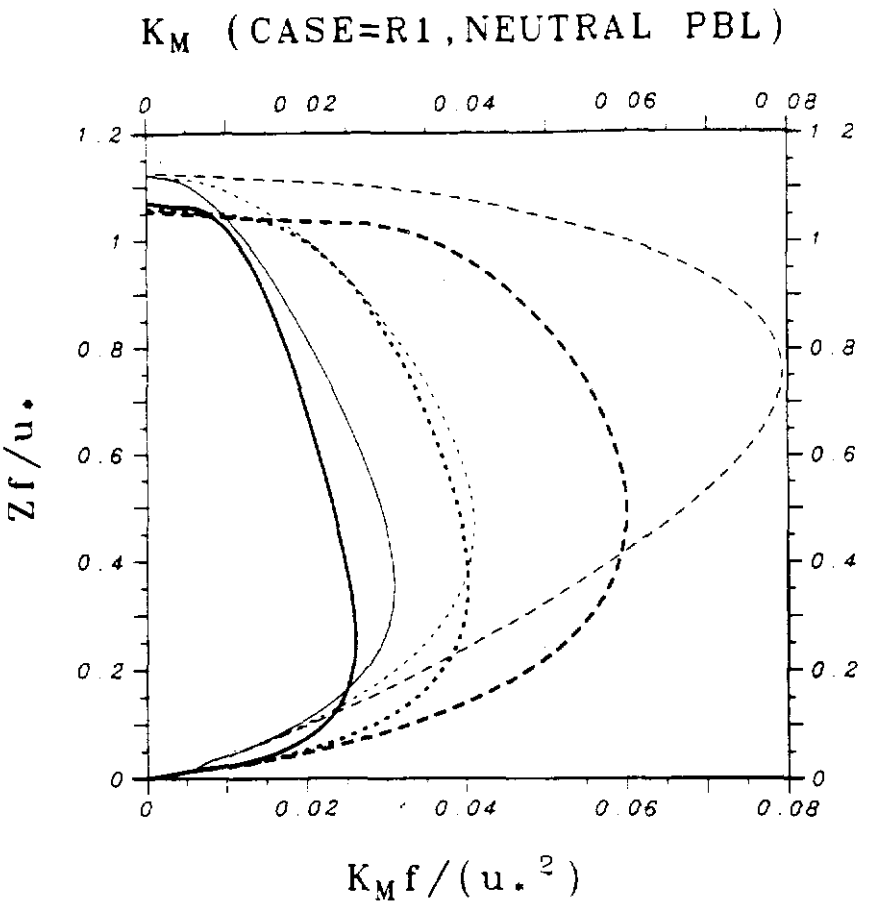

Fig. 2. As in Figure 1 except for the normalized eddy diffusivity for momentum ($K_M f/u_*^2$).

Note that an increase in the master-length (see Equation (A16)) coefficient α (see bold dashed lines) results in proportionally increased l and thus K_M, indicating the importance of this coefficient. The model results for the maximum normalized eddy diffusivity ($K_M f/u_*^2$) in a neutral PBL (see Table I) are comparable to those of LES and higher-order closure models which give maximum values in the range of 0.02–0.03 at a nondimensional height of 0.2–0.3 (e.g., Deardorff, 1972; Wyngaard *et al.*, 1974). Based on Table I, $\alpha \approx 0.05$ and $\beta \approx 2$ are optimal to obtain the most consistent results. The background dissipation added at upper levels helps to limit the abnormal increase of eddy mixing for KL, and the results are now similar to those given by BL.

Vertical distributions of the normalized TKE ($E/c_1 u_*^2$) are shown in Figure 3. The computed TKEs decrease somewhat linearly with height and tend to vanish at a normalized height of about 1.1. They are not observed to vanish at a normalized height of 0.6 which is often found in higher-order closure model results.

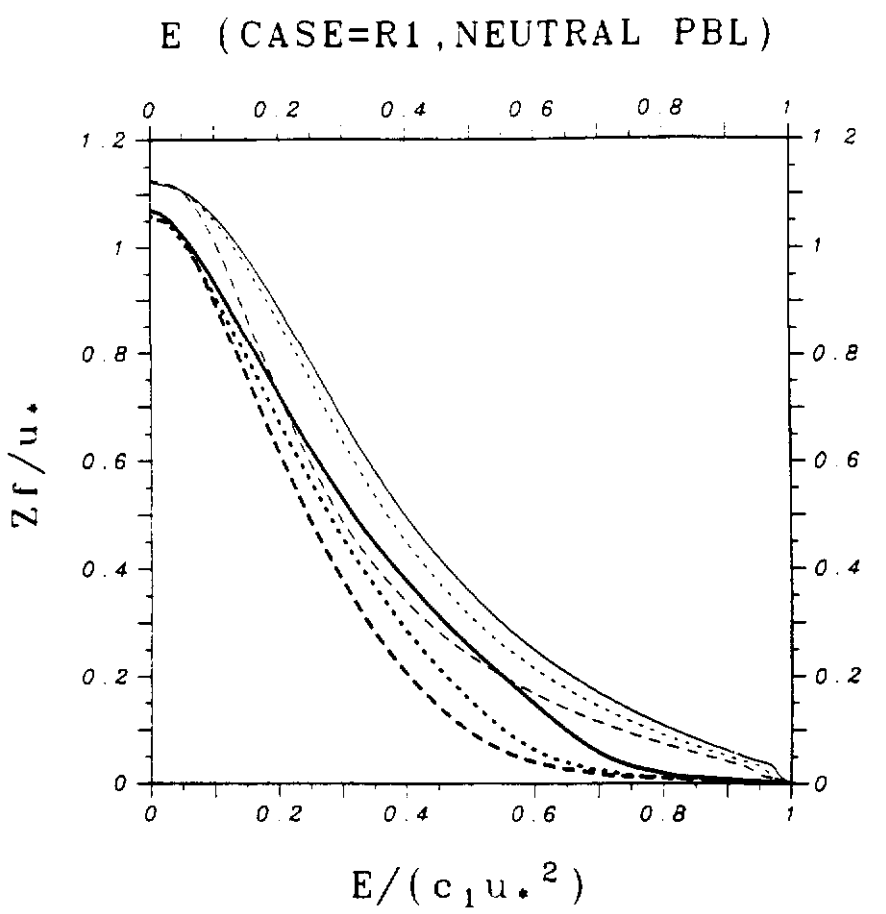

Fig. 3. As in Figure 1 except for the normalized TKE ($E/c_1u_*^2$).

The TKE profiles are consistent with the K_M profiles shown in Figure 2. It should be noted that the model results pertain to the steady-state solution, which takes about 4–6 days of integration. The TKE profiles at 12 h are closer to other higher-order closure or LES model results. At steady state, the normalized TKE is not significantly sensitive to the formulations, BL, KL or the modified KL and to changes in α. But, the actual TKE-profiles for a given geostrophic flow would be sensitive to eddy mixing length (Arya, 1988).

The TKE budgets for BL with $\alpha = 0.1$ (bold lines) and KL with $\beta = \infty$ (thin lines) are quite similar (Figure 4). In a neutral boundary layer, the shear production of TKE is primarily balanced by its dissipation, and turbulent transport is almost negligible except at the upper levels. Near the surface, BL shows small positive turbulent transport (bold long dashed), while KL (thin long dashed) gives small negative values. The turbulent transport in the lower portion of a neutral PBL

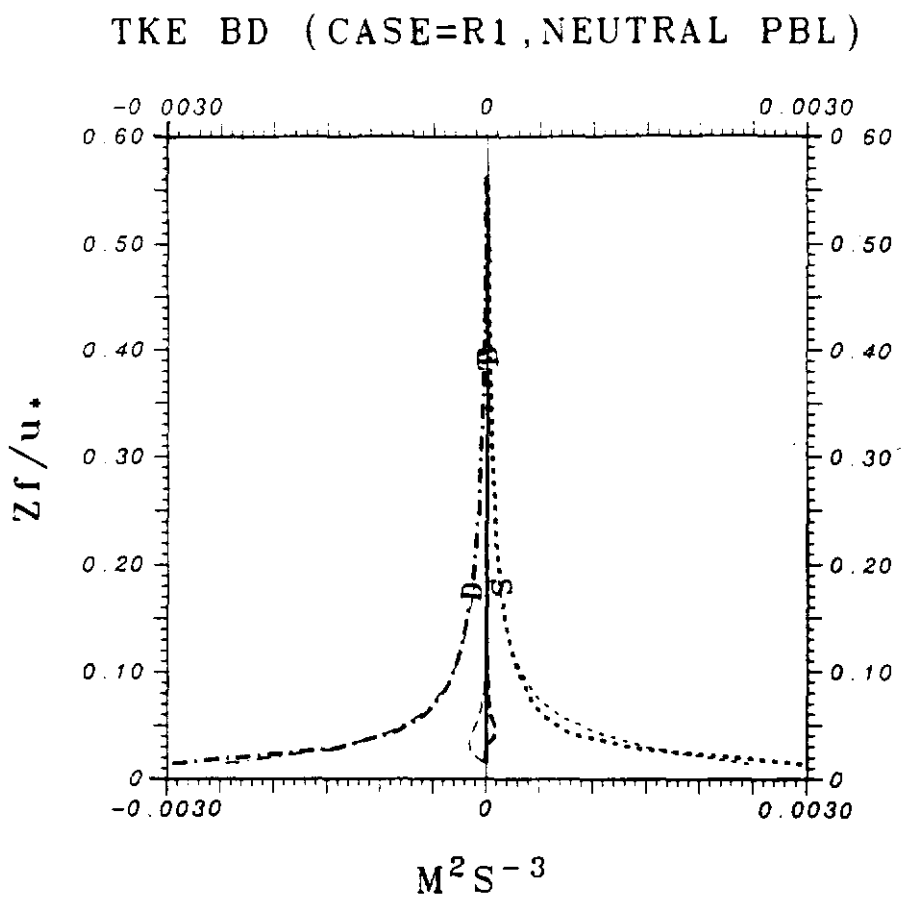

Fig. 4. Vertical profiles of turbulent kinetic energy (TKE) budgets for a neutral PBL (case R1). Bold lines are for the modified Blackadar formulation (with $\alpha = 0.1$) and thin lines for Kolmogorov's formulation (with $\beta = \infty$). TKE budgets are buoyancy (solid lines), shear production (shorter dashed), turbulent transport (longer dashed) and dissipation (dotted-dashed).

thus is less important as compared to the other two contributions, shear production and dissipation. Note that all the TKE budget components decay to zero at a height of about 0.6 and to 1% of their surface values at a height of about 0.4. Although a neutral PBL rarely exists in the atmosphere, limited observations (Nicholls, 1985) and higher-order closure results show that the TKE budgets in a neutral PBL rapidly decay with height, with slight negative turbulent transport within a nondimensional height of 0.1 as found in the present study. Comparing the TKE profiles and budget components, one may conclude that turbulent transport at the upper levels of a neutral PBL is more difficult to model, since it becomes relatively more important but sensitive to the upper boundary conditions. Only turbulent transport (at the equilibrium stage) can explain the existence of significant TKE for $fz/u* > 0.3$.

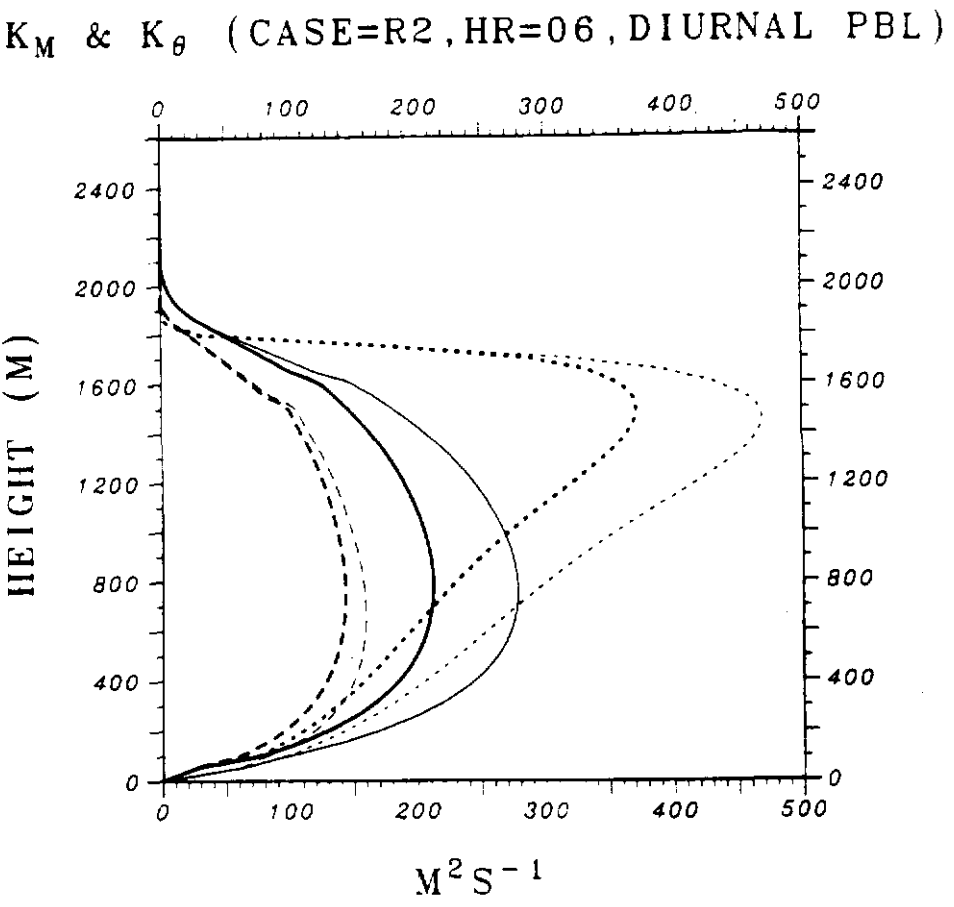

Fig. 5. Vertical profiles of K_M (bold lines) and K_θ (thin) at 6 h for case R2 (a diurnal PBL) using different eddy diffusivity closures: the level 2.5 using the modified Blackadar's formulation with $\alpha = 0.1$ (solid line) and Kolmogorov's formulation with $\beta = \infty$ (shorter dashed) and the E-model with a simple formulation for the Prandtl number (longer dashed). See text for details.

3.2. Diurnal PBL

Diurnal surface temperatures are specified in R2 using a sinusoidal function with a maximum warming amplitude of 20°C. The diurnal cycle of surface heating starts at 0 model hour.

Figures 5 and 6 show the results for the profiles of K_M (bold lines) and K_θ (thin lines) at 6 and 12 h, respectively, for the E-ϵ model with BL (solid) and KL (dashed) and for the E-model (long dashed). Note that in this model, Equation (A8) is used to account for the eddy Prandtl number which may be influenced by thermal stability. It is obvious from Figure 5 that the E-ϵ model with KL exhibits unreasonably large eddy diffusivities in the entrainment region near the top of the PBL at 6 h. At this time, the PBL has developed to a height of about 2 km, with eddy diffusivities in the range of 200–300 $m^2 s^{-1}$. It can be seen that the eddy

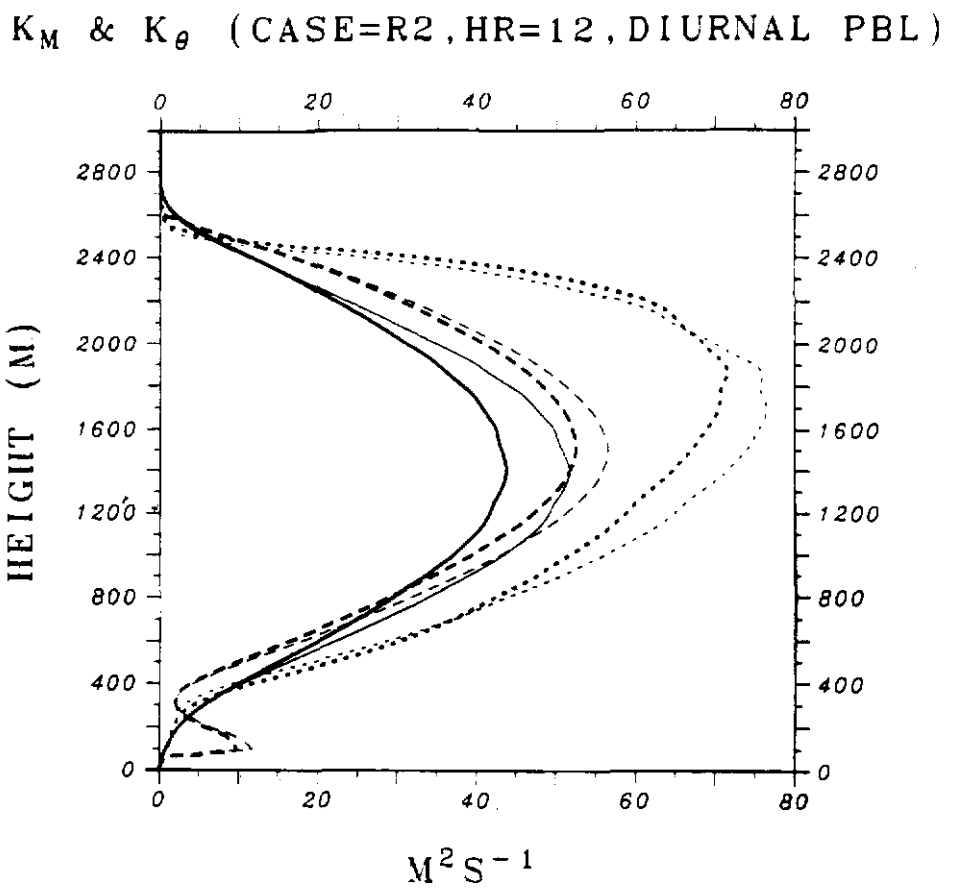

Fig. 6. As in Figure 5 but at 12 h.

diffusivities at the mid-PBL for the E-model are somewhat less than those in the level 2.5 run. The PBL height continuously rises and develops to about 2800 m at 12 h (at this time the surface layer is stable), while the magnitudes of eddy diffusivities drop to values below 100 $m^2 s^{-1}$ (Figure 6). At 12 h, the E-ϵ model with KL also yields larger eddy diffusivities at the upper levels as compared to BL, but the results are less abnormal than at 6 h. On the other hand, the E-model run at 12 h gives larger eddy diffusivities than those in the level 2.5 run, indicating that the coefficient c_2 in (A6) is probably not a constant. Besides, the E-model run also gives maximum eddy diffusivities at lower altitude as compared to those in the other two model runs. This could be due to the overweighting in (A8) for a stable surface layer.

Figure 7 shows the variation of maximum P_{rt} above the surface layer for the E-ϵ model with BL (solid) and the E-model (dashed). Around the time of maximum surface heating (6 h), the maximum P_{rt} for the E-model is somewhat larger than that for the E-ϵ model, but their evolutions are similar. The results using the

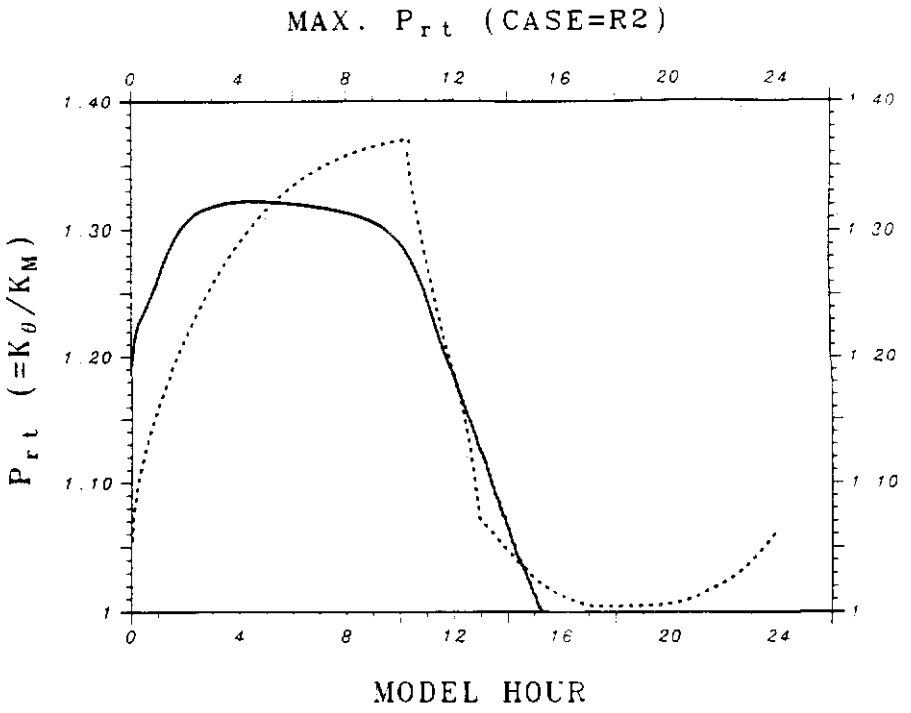

Fig. 7. Variation of the maximum Prandtl number above the surface layer with time for the level 2.5 formulation with $\alpha = 0.1$ (solid line) and the modified E-model (dashed) for case R2.

simpler E-model are encouraging as compared to the results using other closure models.

As shown before, the E-ϵ model with KL tends to yield excessively large eddy diffusivities, particularly at 6 h (the most unstable surface layer). Figure 8 shows the eddy mixing lengths at 6, 12, 18 and 24 h for the BL and KL runs. Large eddy mixing lengths (exceeding 1000 m at 6 and 12 h) are found near the top of the PBL for the KL run. However, the eddy mixing lengths at the lower levels of the PBL are similar for the two runs. In the entrainment region, the KL run has a mixing length several orders larger than in the BL run, while their predicted PBL heights are about the same.

Comparing Figures 5, 6 and 8, one can find that the computed eddy diffusivities are not proportional to increases in eddy mixing length. This is because $K_M = c_2 l E^{1/2}$ with a deterministic factor, $E^{1/2}$. Figure 9 shows the TKE profiles for the KL and BL runs. It can be seen that their predicted TKEs are quite similar, showing a typical CBL at 6 h and NBL at 18 and 24 h. The influence of significantly large l on K_M at 6 h for the KL run is offset by the small TKE in the entrainment region. The similarity between the TKE profiles obtained using the BL and KL formulations is encouraging. It is interesting to note that the E-ϵ model with KL

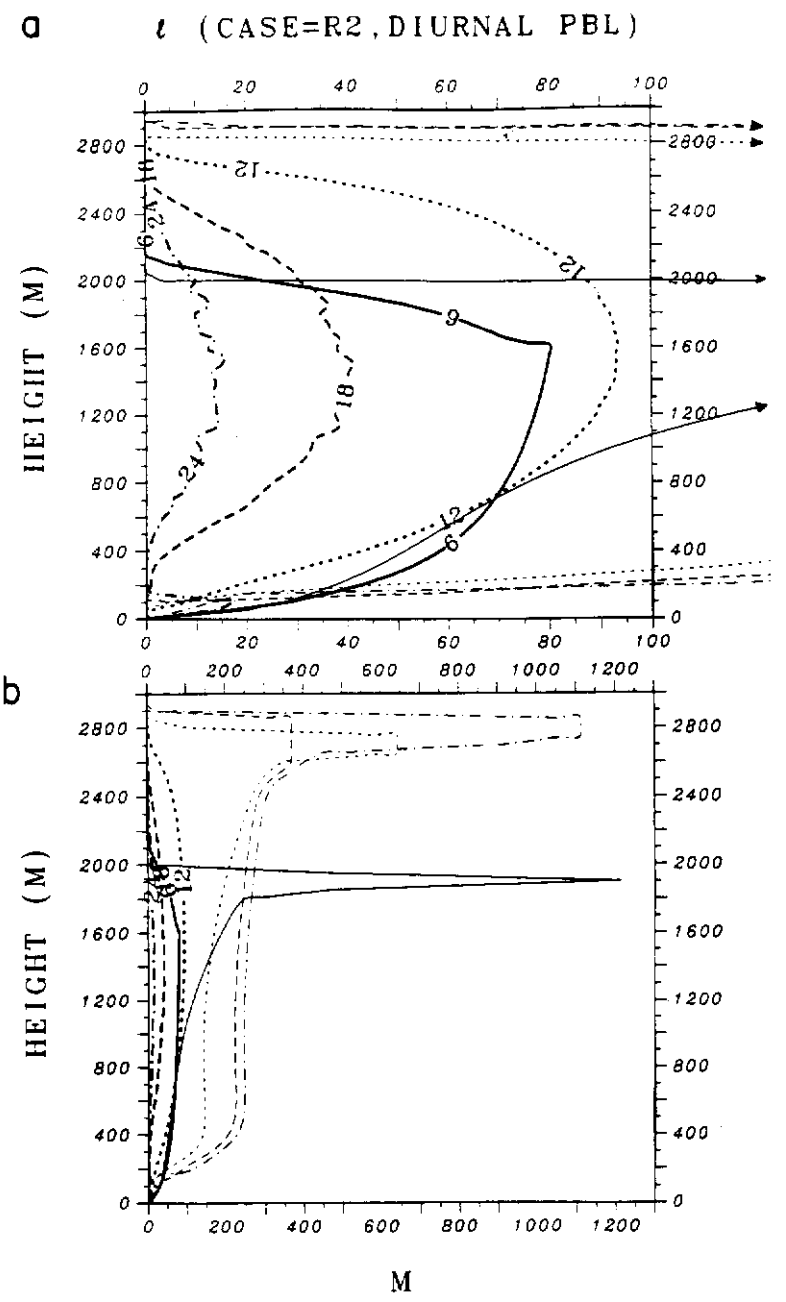

Fig. 8. Eddy mixing lengths at 6 (solid lines), 12 (shorter dashed), 18 (longer dashed) and 24 h (dotted-dashed) for case R2 using different mixing-length formulations, the modified Blackadar formulation with $\alpha = 0.1$ (bold) and Kolmogorov's formulation $\beta = \infty$ (thin).

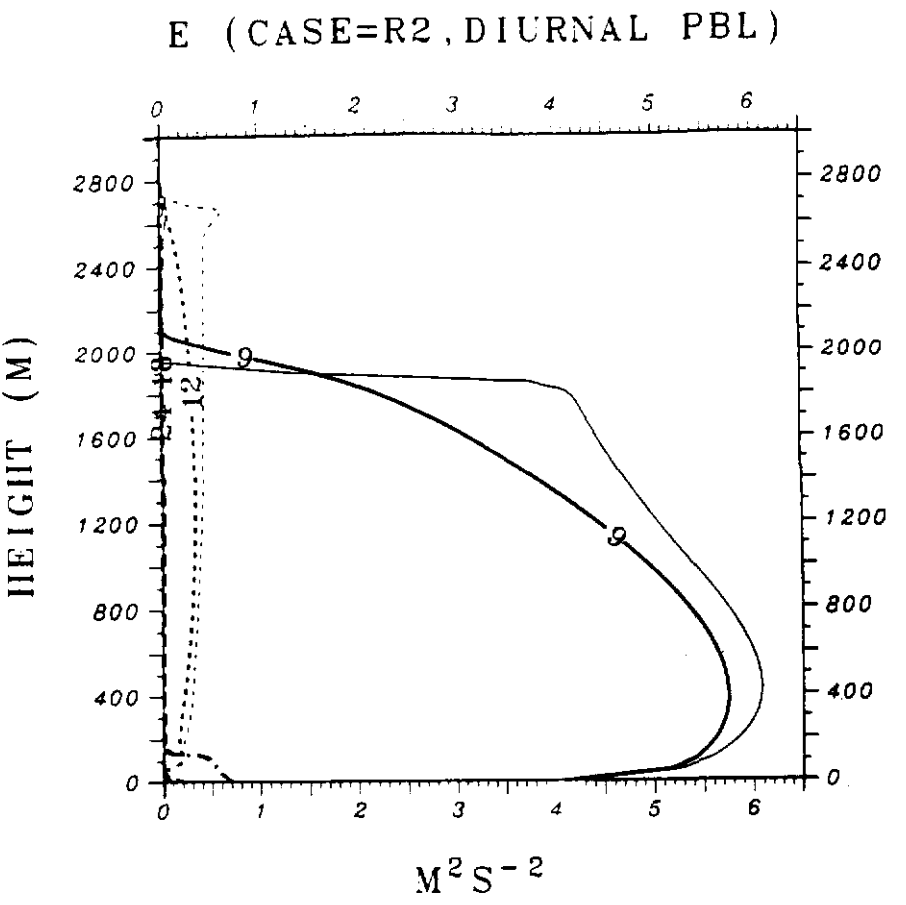

Fig. 9. As in Figure 8 but for TKE.

could adjust itself to avoid overpredicting the turbulence intensity even when the associated eddy mixing length is unreasonably large.

With similar distributions of the TKE and similar PBL heights, the BL and KL runs yield very similar profiles of u, v and θ within the PBL (Figures 10, 11 and 12), except in the entrainment region. A low-level jet is simulated at 18 and 24 h. At night, a near-neutral layer (residual layer) up to 2.8 km is produced by the two runs. This layer has very small TKE above the stable surface layer and persists for a long time. For this case, nocturnal radiational cooling would help to reset the mean structure to that of the previous day (André *et al.*, 1978). Besides, turbulence closures assuming down-gradient transport (like the E-ϵ model) probably are incapable of modeling a NBL following a CBL. Higher-order closures that directly predict turbulent moments do not suffer from this disadvantage.

The entrainment regions for the BL and KL runs can be better seen in their TKE budgets (Figure 13). For comparison, the E-model results are also given in the figure. It is obvious that all three runs give very similar distributions of TKE

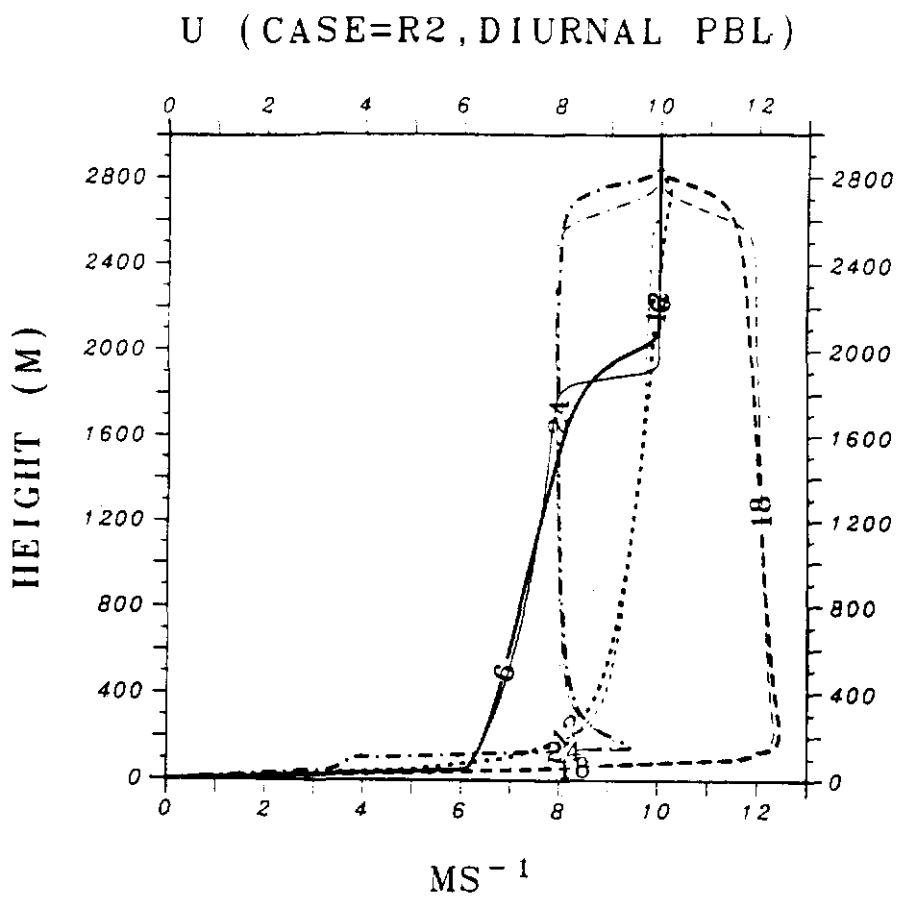

Fig. 10. As in Figure 8 but for u.

budgets. Again, the E-ϵ model with KL exhibits larger entrainment effects at about 1.9 km height, evident in the larger magnitude of turbulent transport (thinner longer dashed line). All three runs show the entrainment intensity (represented by negative buoyancy) to be about 15–20% of the magnitude of surface buoyancy production. The TKE budgets for the three runs compare well with the level 3 closure (e.g., Sun and Ogura, 1980) and with the LES results for a typical CBL (Moeng and Wyngaard, 1989).

3.3. Convective MBL

Convective MBL is often observed over the ocean when the sea surface temperature (SST) is warmer than air temperature. Diurnal SST variations are often negligible for short time periods. In this case (R3), the SST is thus assumed to be constant since the total integration time is only 12 h. Surface roughness is determined by Charnock's relationship.

With the initial 20°C air-sea temperature difference observed during a severe

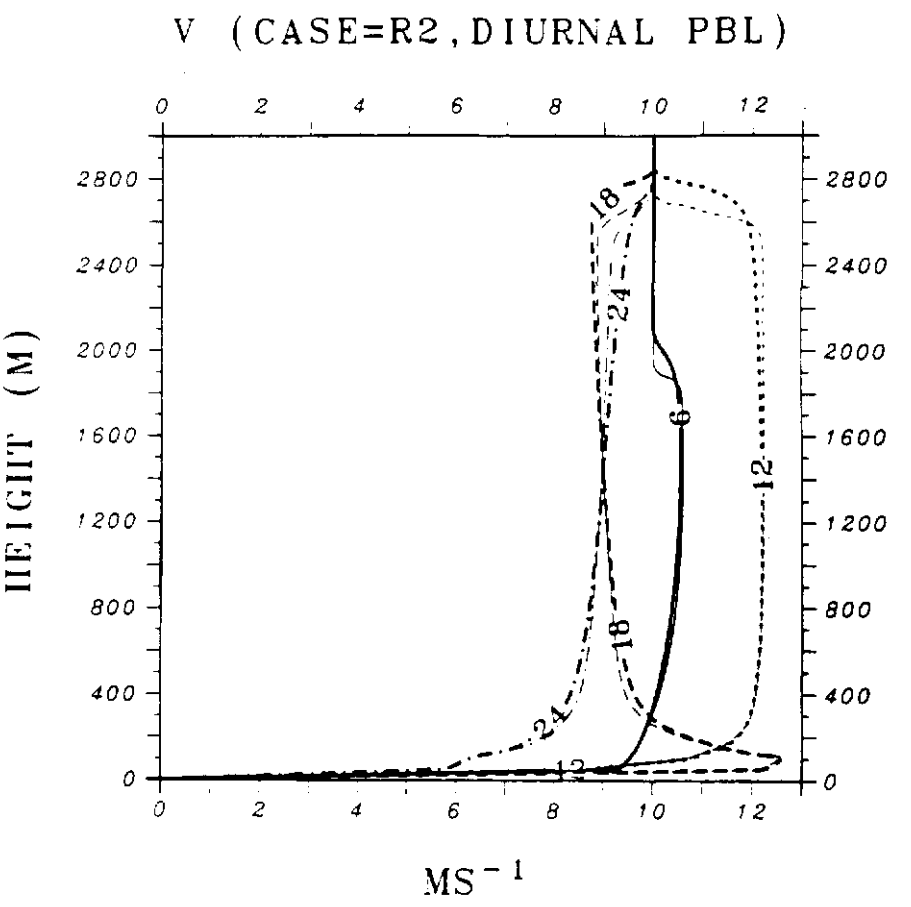

Fig. 11. As in Figure 4 but for v.

cold air outbreak over the Gulf Stream (Wayland and Raman, 1989), the MBL can develop to 2.5 km at 6 h and 3.1 km at 12 h, as evident in Figure 14 for eddy diffusivities and in Figure 15 for TKE. Magnitudes of maximum eddy diffusivities are about 200–300 $m^2 s^{-1}$ at 6 h increasing to 300–400 $m^2 s^{-1}$ at 12 h; the maximum TKE is 4.5 $m^2 s^{-2}$ at 6 h increasing to about 5.1 $m^2 s^{-2}$ at 12 h. Comparing Figure 15 to Figures 5 and 9, one sees that the distributions of TKE and eddy diffusivities in the convective MBL are similar to those in the CBL over land.

Figure 16 shows the profiles of TKE budgets for the convective MBL (case R3). In response to the warm surface, positive buoyancy decreases linearly with height, as observed in a typical CBL. Associated with the highly convective MBL is a significant entrainment region near the 2 km height at 6 h, which is lifted to about 3.1 km at 12 h. Negative heat fluxes equal to about 20% of surface buoyancy are activated by the turbulent entrainment across the boundary between the upper stable and the underlying unstable layers. Within the entrainment region, negative buoyancy and dissipation are compensated by positive turbulent transport. Shear

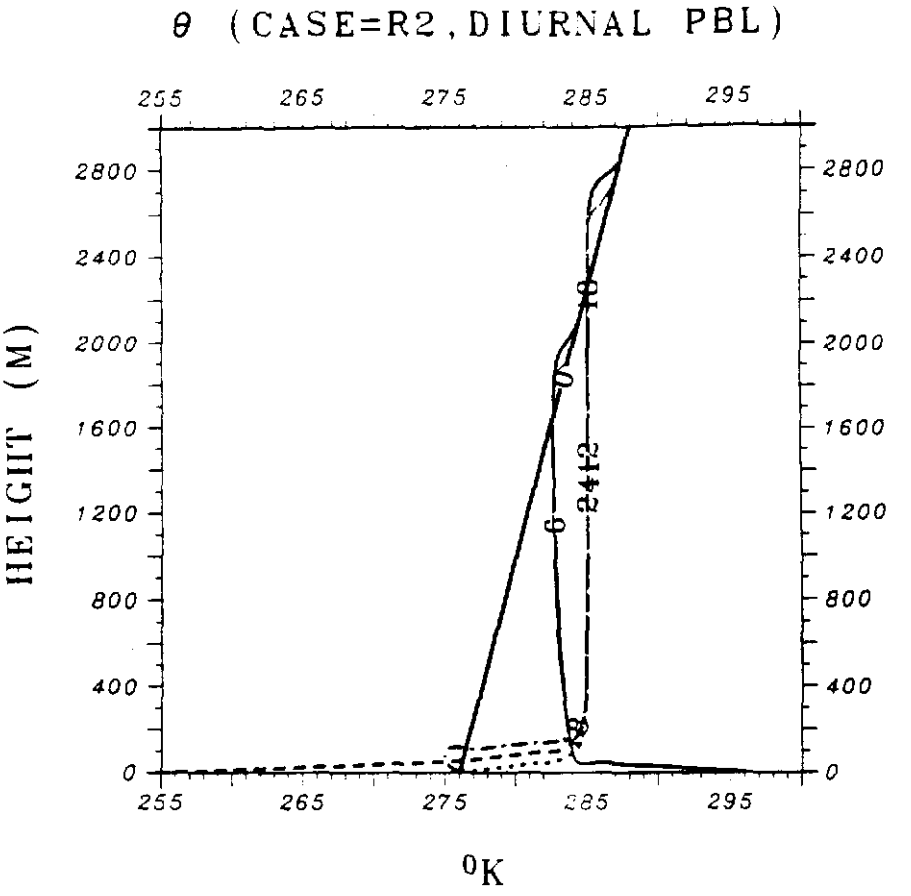

Fig. 12. As in Figure 8 but for θ.

production is important only near the surface where turbulent transport is negative. The crossover points of turbulent transport and buoyancy are near the nondimensional heights of 0.6 and 0.8, respectively.

4. Discussions

4.1. Eddy mixing length

Some investigators (e.g., Mellor and Yamada, 1982; Yamada, 1983) tended to use a prognostic equation for the eddy mixing length rather than one for turbulent dissipation to parameterize eddy diffusivities. The PBL has a typical height of about 1 km and thus the size of largest eddies will be of the same order of magnitude. In contrast, turbulent dissipation is a locally isotropic microscale-process. Since energy-containing eddies have much larger length scales than turbulent dissipation, one has to be careful in the parameterization of eddy diffusivity in terms of turbulent dissipation.

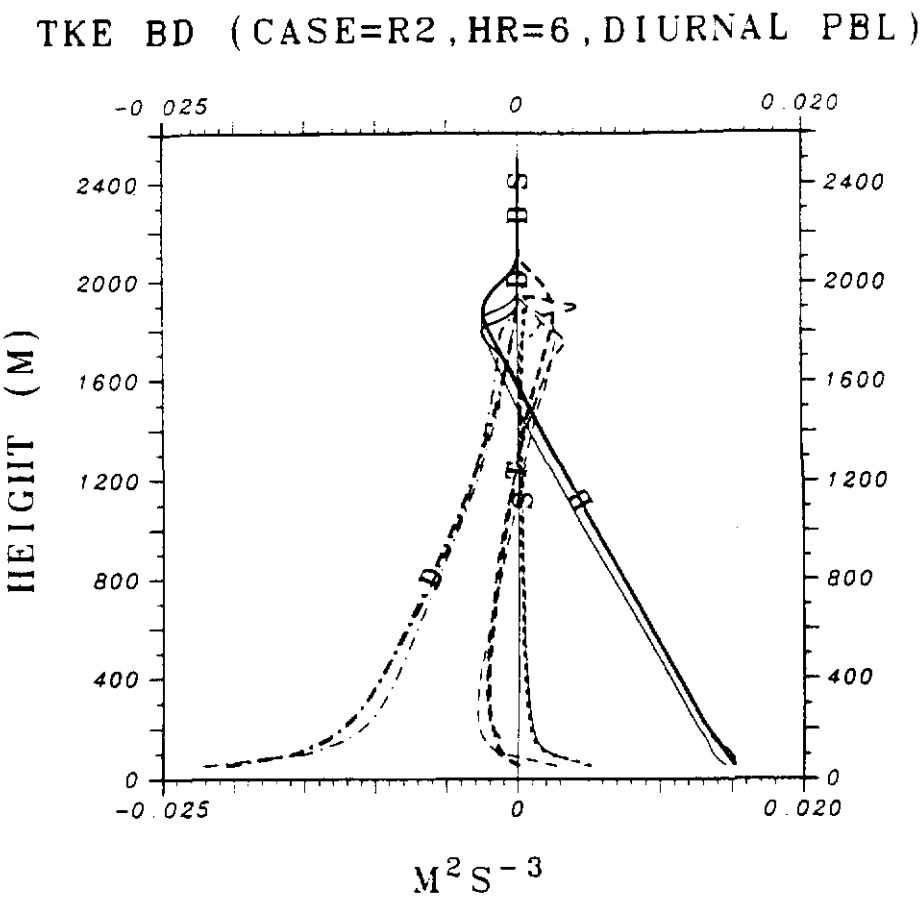

Fig. 13. Vertical profiles of TKE budgets at 6 h for case R2 using different closures: the level 2.5 one using the modified Blackadar formulation with $\alpha = 0.1$ (heaviest lines) and Kolmogorov's formulation with $\beta = \infty$ (heavier), and the modified E-model (thinnest).

The KL formulation does not necessarily need a weighting on the part of turbulent mixing due to the wall effects (e.g., Detering and Etling, 1985; Duynkerke, 1988). Using the KL formulation, the E-ϵ model is free of several presumed length scales such as l_0, l_s and l_N required for BL. A major problem in this E-ϵ model is the singularity that exists in KL and probably in the ϵ-equation since the factor E/ϵ in (A21) is usually overpredicted at the upper levels of the PBL. Apparently, this ratio (as a time scale) is hard to model accurately as both E and ϵ become very small. The problem has been clearly illustrated in the results for case R2 (diurnal PBL) in the previous section. In this study, the method using background dissipation to control the factor E/ϵ was found helpful in avoiding the singularity in the E-ϵ model.

The BL formulation does not have singularity because eddy mixing length is mathematically bounded by several length scales. However, BL has the disadvan-

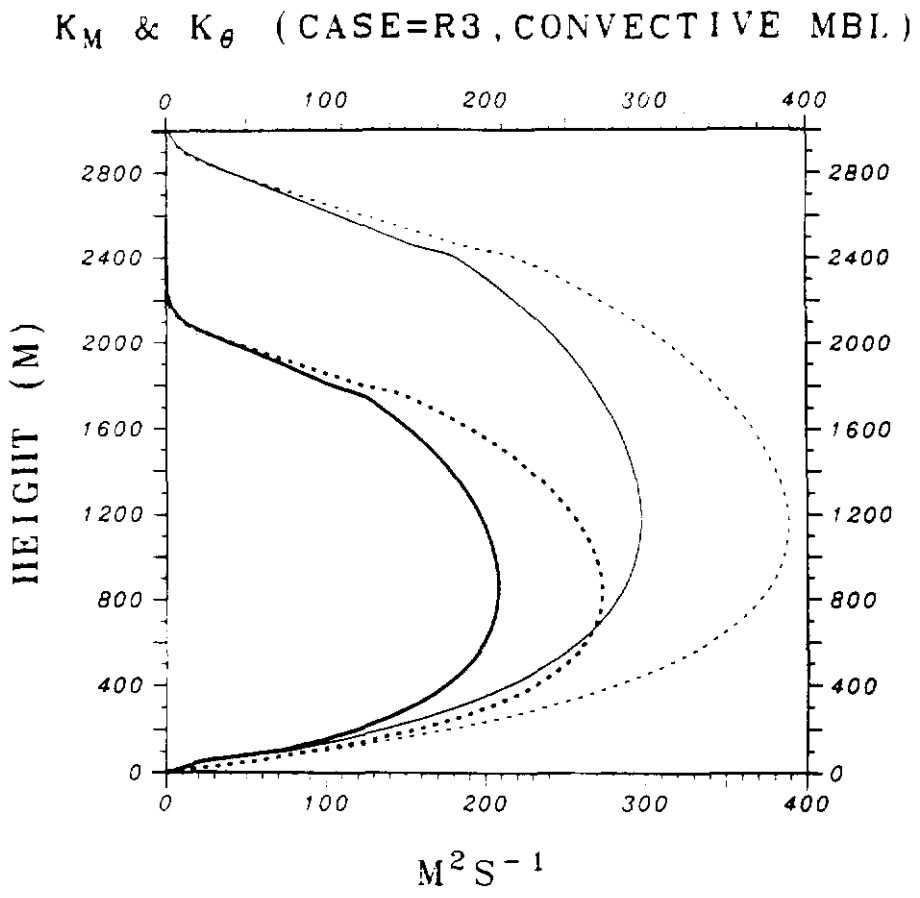

Fig. 14. Vertical profiles of K_M (solid lines) and K_θ (dashed) at 6 (bold) and 12 (thin) h for case R3 (a convective marine boundary layer).

tage of requiring several presumed length scales, most significantly, the master-length scale (see Equation (A16)) with a coefficient α that is not well known. It was shown in the previous section that the master length coefficient α significantly affects the magnitude of eddy diffusivities for R1 (a neutral PBL). As seen in Table I, this coefficient also changes the eddy diffusivities considerably in a convective MBL. For example, the maximum magnitudes of K_M at 6 and 12 h are almost doubled as α doubles. Optimum value for this coefficient cannot be determined without observational evidence.

4.2. The lower boundary conditions of TKE and dissipation

The TKE at the lowest model level is determined by (A23). A zero gradient condition for the TKE at the lowest layer (the surface layer) is not appropriate in modeling a PBL in transition since the changing lower boundary effects are important. In using (A23), which requires Kolmogorov's assumption for turbulent

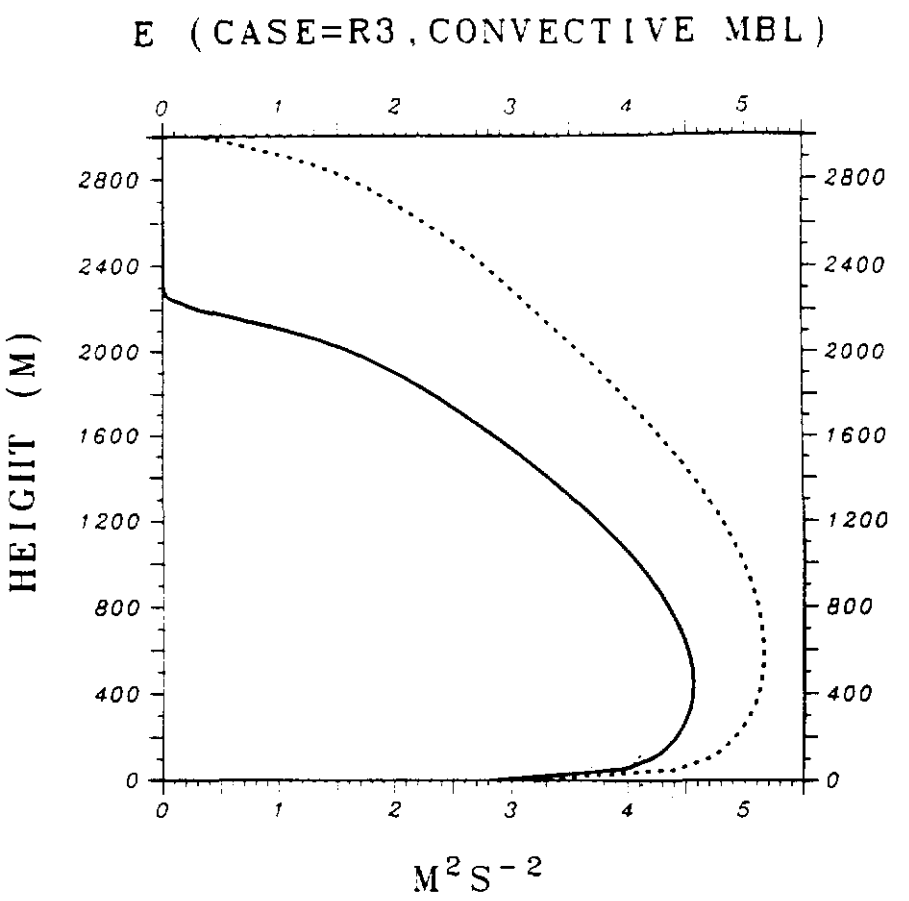

Fig. 15. As in Figure 14 but for TKE.

dissipation, the parameter c_w in part determines the TKE. It can be seen from Table I that with $c_w = 0$, a ratio of maximum domain and surface TKEs exceeding 3 is obtained for R3, while with $c_w = 0.2$ this ratio reduces to about 1.6. The surface-layer friction velocity ($u*$) and convective velocity ($w*$), however, are little influenced by the change in c_w. Heights of the MBL are also similar for $c_w = 0$ and $c_w = 0.2$. The LES results (Moeng and Wyngaard, 1989) indicate this ratio to be below 2 for a typical $w*$ of 2–3 m s^{-1}.

The lowest layer of computed ϵ in the model is the surface layer (not the surface) because using (A24) the turbulent dissipation becomes infinite at the surface. In the surface layer, an equilibrium stage of turbulence is assumed in order to specify the dissipation. Thus, all the E-ϵ model results predict relatively small turbulent transport in the surface layer. For the convective PBL, this lower boundary condition for turbulent dissipation seems to work equally well as compared to the E-model results using Kolmogorov's hypothesis.

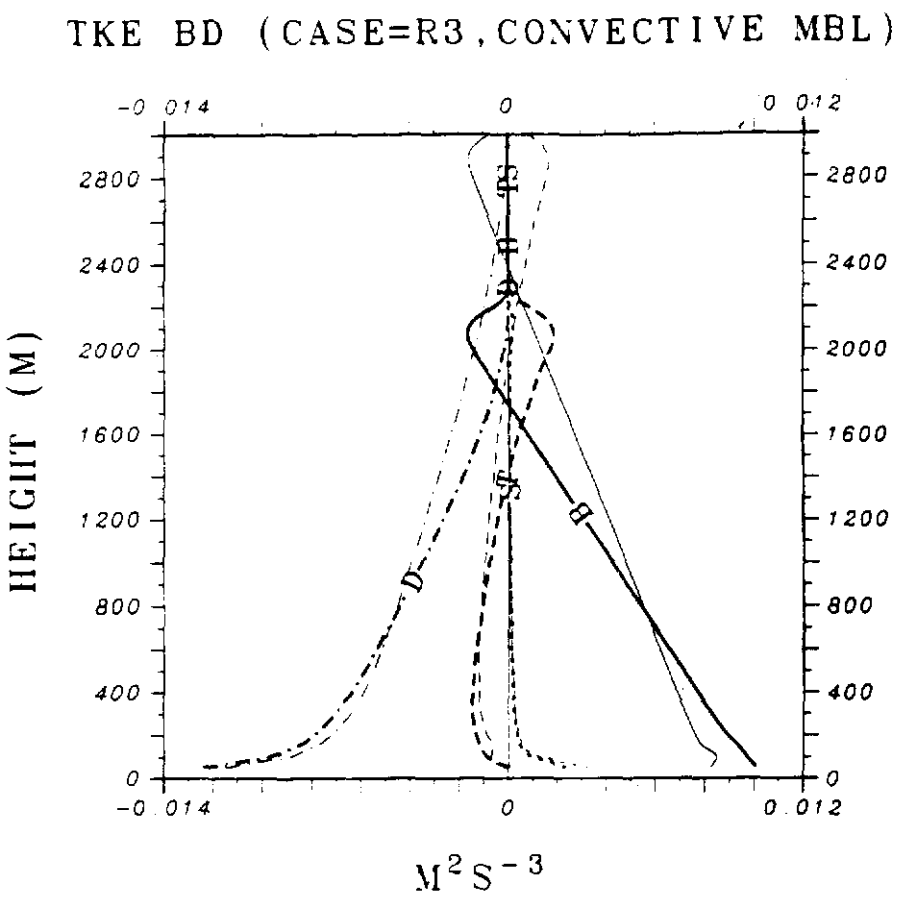

Fig. 16. As in Figure 14 but for TKE budgets: buoyancy (solid lines), shear production (shorter dashed), turbulent transport (longer dashed) and dissipation (dotted-dashed).

4.3. The eddy Prandtl number

The influence of the eddy Prandtl number would increase as the turbulence becomes more intense in convective conditions. The level 2.5 closure includes the effects of stability and shear to determine eddy Prandtl number, using more complicated formulations derived from the level 4 of second-order closure (Mellor and Yamada, 1982). As shown previously, the influence of the Prandtl number in the 1-D PBL flow appears to be minor, despite large differences in the predicted magnitudes of eddy diffusivities for momentum and heat. It is speculated that this difference is limited for the 1-D convective and stable PBL flow, because for the former the flow is well mixed and depends only on the development of the PBL height and for the latter the turbulence is suppressed by the stable stratification at upper levels. For the same TKE equation, the resulting differences due to different mixing-length formulations are small, particularly, for the convective

flow, as evident in Figures 10, 11 and 12. The 1-D modeling tests do not show an important role of the Prandtl number in changing the PBL structure. (It will be demonstrated in Part II that the specification of the Prandtl number is significant for the multi-dimensional flow over the Gulf Stream region when clouds are present and interact with the MBL.)

5. Conclusions

Turbulence closures using the turbulent kinetic energy (TKE) and dissipation (ϵ) equations are investigated with emphasis on flow sensitivities to different eddy mixing-length formulations. In the E-ϵ closure, the level 2.5 one of Mellor and Yamada (1982) has been implemented for better determination of the eddy diffusivities for momentum and heat. One-dimensional (1-D) model results show that the PBL flows under various stability conditions are not significantly sensitive to Blackadar's and Kolmogorov's formulations, although the latter yields excessively large eddy mixing lengths in the entrainment region of the upper PBL particularly for convective conditions. Even using the more complicated level 2.5 formulation, the E-ϵ model prediction shows no noticeable superiority to the economical E-model which uses only the TKE equation and a simple relation for the ratio between eddy diffusivities for momentum and heat (i.e., the eddy Prandtl number). Similar predictions of the mean fields and the turbulent moments for the different closure assumptions can be attributed to the fact that global similarity is assured by the use of the same TKE equation. For example, large TKE in the entrainment region is not produced by excessively large eddy mixing lengths given by Kolmogorov's formulation. The influence of the eddy Prandtl number therefore is not apparent in the 1-D flow tests.

Acknowledgments

We wish to thank Dr. S. P. S. Arya for several helpful suggestions. This work was supported by the Division of Atmospheric Sciences, National Science Foundation under grant ATM-88-01650.

Appendix. The Turbulence Closures

The TKE equation is given by (in the z-coordinate)

$$\frac{\partial \mathrm{E}}{\partial t} = \underbrace{-\mathbf{V}\cdot\nabla \mathrm{E}}_{\mathbf{A}} + \underbrace{\left[-\overline{u'w'}\frac{\partial u}{\partial z} - \overline{v'w'}\frac{\partial v}{\partial z}\right]}_{\mathbf{S}} + \underbrace{\frac{g}{\theta_0}\overline{w'\theta_v'}}_{\mathbf{B}} - \underbrace{\frac{\partial \overline{w'(\mathrm{E}' + p'/\rho_0)}}{\partial z}}_{\mathbf{T}} - \underbrace{\epsilon}_{\mathbf{D}} \qquad \text{(A1)}$$

where primed variables represent fields at subgrid scale. The TKE budget components consist of advection (term A), shear production (term S), buoyancy (term

B), turbulent transport (term **T**) and turbulent dissipation (term **D**). Following Deardorff (1980) closely, eddy fluxes are parameterized as

$$\overline{u'w'} = -\mathrm{K}_M \frac{\partial u}{\partial z}, \tag{A2}$$

$$\overline{v'w'} = -\mathrm{K}_M \frac{\partial v}{\partial z}, \tag{A3}$$

$$\overline{w'(\mathrm{E}' + p'/\rho_0)} = -c_T \mathrm{K}_M \frac{\partial \mathrm{E}}{\partial z}, \tag{A4}$$

$$\overline{w'\theta_v'} = -(1 + 0.61\,q - q_l)\mathrm{K}_\theta \frac{\partial \theta}{\partial z} - (0.61\theta)\mathrm{K}_q \frac{\partial q}{\partial z} + \theta\,\mathrm{K}_q \frac{\partial q_l}{\partial z}, \tag{A5}$$

$$\mathrm{K}_M = c_2 l\,\mathrm{E}^{1/2}, \tag{A6}$$

and

$$\mathrm{K}_\theta = \mathrm{P}_{rt}\mathrm{K}_M \tag{A7}$$

where in (A5) the total liquid water q_l is the summation of cloud water (q_c) and rain water (q_r) and in (A7), P_{rt} is the inverse eddy Prandtl number. Model results based on large-eddy simulations (LES) tend to indicate that the average inverse eddy Prandtl number rarely exceeds 2 even for the turbulence in convective storms (e.g., Redelsperger and Sommeria, 1986). Thus, the inverse eddy Prandtl number is determined in this study as

$$P_{rt} = \text{Minimum of } [3.,(1 + c_l l/l_1)] \tag{A8}$$

where l is eddy mixing length, l_1 the mixing length predominantly influenced by the wall (defined later) and c_l a constant coefficient.

A better determination of P_{rt} is given in the level 2.5 formulation, a simplified version of the level 4 one (Mellor and Yamada, 1974, 1982). The level 2.5 closure contains the same prognostic TKE equation, but has complicated formulations for eddy diffusivities K_M and K_θ. The final forms for K_M and K_θ in the level 2.5 formulation after considerable algebraic reduction can be expressed as

$$\mathrm{K}_M = c_2 l\,(2\mathrm{E})^{1/2}\mathrm{S}_M, \tag{A9}$$

$$\mathrm{K}_\theta = c_2 l\,(2\mathrm{E})^{1/2}\mathrm{S}_H, \tag{A10}$$

where S_M and S_H are obtained from

$$S_M[6A_1A_2G_M] + S_H[1 - 3A_2B_2G_H - 12A_1A_2G_H] = A_2$$

$$S_M[1 + 6A_1^2G_M - 9A_1A_2G_H] - S_H[12A_1^2G_H + 9A_1A_2G_H] = A_1(1 - 3C_1)$$

with

$$G_M = \frac{l^2}{2E}\left[\left(\frac{\partial u}{\partial z}\right)^2 + \left(\frac{\partial v}{\partial z}\right)^2\right] \tag{A11}$$

and

$$G_H = -\frac{l^2}{2E}\frac{g}{\theta}\frac{\partial \theta_v}{\partial z}. \tag{A12}$$

Mellor and Yamada (1982) set the constants $(A_1, A_2, B_2, C_1) = (0.78, 0.79, 8.0, 0.056)$ and assumed $G_H \leqslant 0.033$ and $G_M \leqslant 0.825 - 25\,G_H$ to reduce some singularities existing in the level 2.5 closure because of the level simplification. Helfand and Labraga (1988) have formulated a non-singular version of the level 2.5 formulation, but this version sacrifices some features of the original one due to additional constraints imposed on the closure coefficients.

The mixing length l is still unknown and needs to be parameterized in terms of the known variables. It is formulated under different stability conditions such that for stable conditions, $\partial\theta_v/\partial z > 0$,

$$l_s = 0.76\,E^{1/2}\left[\frac{g}{\theta_0}\frac{\partial \theta_v}{\partial z}\right]^{-1/2} \tag{A13}$$

and for neutral or unstable conditions, $\partial\theta_v/\partial z \leqslant 0$,

$$\frac{1}{l_N} = \frac{1}{l_1} + \frac{1}{l_0} \tag{A14}$$

where

$$l_1 = k(z + z_0) \tag{A15}$$

and l_0 the master (or primary) length scale is defined as

$$l_0 = \alpha\frac{\int_0^H E^{1/2}\,z\,dz}{\int_0^H E^{1/2}\,dz}, \tag{A16}$$

where α is a constant coefficient on the order of 0.1. To induce a smooth change

for the mixing length from neutral conditions to slightly stable conditions, the stable mixing length is modified as

$$\frac{1}{l} = \frac{1}{l_1} + \frac{1}{l_0} + \frac{1}{l_s}, \tag{A17}$$

while the unstable mixing length $l = l_N$. Similar formulations for l were used by many investigators (e.g., André *et al.*, 1978; Sun and Ogura, 1980; Mellor and Yamada, 1982). A review of the eddy mixing-length formulations is given by Holt and Raman (1988).

The TKE dissipation rate, ϵ, can be parameterized using Kolmogorov's hypothesis as

$$\epsilon = c_\epsilon \frac{\mathrm{E}^{3/2}}{l} \tag{A18}$$

where

$$c_\epsilon = c_{\epsilon 1} + c_{\epsilon 2} \frac{l}{k z}. \tag{A19}$$

In the above, $c_{\epsilon 1}$ and $c_{\epsilon 2}$ are constants.

The prognostic equation for turbulent dissipation (ϵ) can be used instead of Kolmogorov's hypothesis. Combination of the TKE and turbulent dissipation equations constitutes the E-ϵ closure. The ϵ-equation is given by (see Duynkerke and Driedonks, 1987)

$$\underbrace{\frac{\partial \epsilon}{\partial t}}_{\mathbf{A}_\epsilon} = \underbrace{-\mathbf{V} \cdot \nabla \epsilon}_{\mathbf{A}_\epsilon} + \underbrace{c_3 \frac{\epsilon}{\mathrm{E}} \left[-\overline{u'w'} \frac{\partial u}{\partial z} - \overline{v'w'} \frac{\partial v}{\partial z} \right]}_{\mathbf{S}_\epsilon} + \underbrace{c_3 \frac{\epsilon}{\mathrm{E}} \frac{g}{\theta_0} \overline{w' \theta'_v}}_{\mathbf{B}_\epsilon} - \underbrace{c_4 \frac{\epsilon^2}{\mathrm{E}}}_{\mathbf{D}_\epsilon} + \underbrace{c_5 \frac{\partial}{\partial z} \mathrm{K}_M \frac{\partial \epsilon}{\partial z}}_{\mathbf{T}_\epsilon} \tag{A.20}$$

where $\mathbf{A}_\epsilon$ is the advection term, $\mathbf{S}_\epsilon$ the shear production term, $\mathbf{B}_\epsilon$ the buoyancy term, $\mathbf{D}_\epsilon$ the dissipation term and $\mathbf{T}_\epsilon$ the turbulent transport term for energy dissipation. In the above, c_3, c_4 and c_5 are closure constants (Duynkerke and Driedonks, 1987; Duynkerke, 1988).

It has been found that the use of the ϵ-equation in a neutral boundary layer results in unreasonably weak turbulent dissipation at upper levels (e.g., Duynkerke, 1988). This is caused by the excessive rate of dissipation consumption ($\mathbf{D}_\epsilon$) and diffusion ($\mathbf{T}_\epsilon$) as compared to dissipation productions due to shear effect **S** and buoyancy forcing **B**.

With the prognostic ϵ, eddy mixing length can be parameterized as

$$l = c_l^{-1/2} \mathrm{E}^{1/2} (\mathrm{E}/\epsilon) \tag{A21}$$

where E/ϵ is regarded as the TKE dissipation time scale. Note that use of (A21) is equivalent to use of (A18) for turbulent dissipation in the TKE closure. Use of

(A21) tends to yield excessively large eddy mixing lengths across the boundary of differing stabilities (e.g., the entrainment region). To remedy this, the dissipation in the factor, E/ϵ, is complemented by the background dissipation defined as

$$\epsilon_0 = \frac{E}{T_0}, \; T_0 = \beta \frac{\int_0^H E \, dz}{\int_0^H \epsilon \, dz} \tag{A22}$$

where β is a constant coefficient. Since the dissipation is very small at the upper levels, this method will prevent an overestimate of eddy mixing length by prescribing a minimum energy dissipation time, T_0.

The boundary condition for TKE is specified as

$$E(z = 0) = c_1 u_*^2 + c_w w_*^2 \tag{A23}$$

where c_w is an adjustable coefficient for the effects of stability. The energy dissipation at the lowest model level can be obtained by neglecting turbulent transport and assuming an equilibrium state in the TKE equation. The boundary condition for ϵ (at the surface layer) thus is

$$\epsilon = \frac{u_*^3}{kz} \phi_M\left(\frac{z}{L}\right) + \frac{g}{\theta_0} (\overline{w'\theta'})_0 . \tag{A24}$$

where $\phi_M(z/L)$ is a nondimensional stability function (see Huang and Raman, 1988).

A time-implicit scheme (Huang and Raman, 1988) for the vertical turbulent transport terms is employed. To compute the vertical gradients of wind and temperature near the surface in the equations for TKE and ϵ more accurately, the surface-layer similarity relationships are combined in the E-ϵ closure, such that

$$S = \frac{u_*^3}{kz} \phi_M\left(\frac{z}{L}\right) \tag{A25}$$

and

$$B = \frac{g}{\theta_0} (-u_* \theta_*). \tag{A26}$$

The updated constants c_3, c_4 and c_5 are given in Duynkerke (1988). In this study, the closure coefficients (c_1, c_2, c_3, c_4, c_5, c_T, c_l) = (5.5, 1, 1.46, 1.83, 0.42, 2, 0.5). During the integration, effects of subgrid eddy mixing are evaluated after the computation of moisture effects. Thus, effects of grid condensation on the vertical mixing are taken into account, but effects of subgrid condensation which probably occurs during eddy mixing are omitted.

References

André, J. C., de Moor, G., Lacarrere, P., Therry, G. and du Vachat, R.: 1978, 'Modeling the 24-hour Evolution of the Mean and the Turbulent Structures of the Planetary Boundary Layer', *J. Atmos. Sci.* **35**, 1861–1883.

Arya, S. P. S.: 1988, *Introduction to Micrometeorology*, Academic Press, San Diego, 303 pp.

Businger, J. A., Wyngaard, J. C., Izumi, Y. and Bradley, E. F.: 1971, 'Flux-Profile Relationships in the Atmospheric Surface Layer', *J. Atmos. Sci.* **28**, 181–189.

Deardorff, J. W.: 1972, 'Numerical Investigation of Neutral and Unstable Planetary Boundary Layers', *J. Atmos. Sci.* **29**, 91–115.

Deardorff, J. W.: 1980, 'Stratocumulus-Capped Mixed Layers Derived from a Three-Dimensional Model', *Boundary-Layer Meteorol.* **18**, 495–527.

Detering, H. W. and Etling, D.: 1985, 'Application of the E-ϵ Turbulence Model to the Atmospheric Boundary Layer', *Boundary-Layer Meteorol.* **33**, 113–133.

Dirks, R., Kuettner, J. P. and Moore, J.: 1988, 'Genesis of Atlantic Lows Experiment (GALE): An Overview', *Bull. Amer. Meteorol. Soc.* **69**, 148–160.

Duynkerke, P. G.: 1988, 'Application of the E-ϵ Turbulence Closure Model to the Neutral and Stable Atmospheric Boundary Layer', *J. Atmos. Sci.* **45**, 865–880.

Duynkerke, P. G. and Driedonks, A. G. M.: 1987, 'A Model for the Turbulent Structure of the Stratocumulus-Topped Atmospheric Boundary Layer', *J. Atmos. Sci.* **44**, 43–64.

Helfand, H. M. and Labraga, J. C.: 1988, 'Design of a Nonsingular Level 2.5 Second Order Closure Model for the Prediction of Atmospheric Turbulence', *J. Atmos. Sci.* **45**, 113–132.

Holt, T. and Raman, S.: 1988, 'A Review and Comparative Evaluation of Multilevel Boundary Layer Parameterizations for First-Order and Turbulent Kinetic Energy Closure Schemes', *Reviews Geophys.* **26** 761–780.

Holt, T., Chang, S. and Raman, S.: 1990, 'A Numerical Study of the Coastal Cyclogenesis in GALE IOP 2: Sensitivity to PBL Parameterizations', *Mon. Wea. Rev.* **118**, 234–257.

Huang, C. Y.: 1990, 'A Mesoscale Planetary Boundary Layer Numerical Model for Simulations of Topographically Induced Circulations', Ph.D. Dissertation Submitted to the Department of Marine, Earth and Atmospheric Sciences, North Carolina State University, Raleigh, 253 pp.

Huang, C. Y. and Raman, S.: 1988, 'A Numerical Modeling Study of the Marine Boundary Layer over the Gulf Stream during Cold Air Advection', *Boundary-Layer Meteorol.* **45**, 251–290.

Huang, C. Y. and Raman, S.: 1989, 'An Application of the E-ϵ Closure Model to Simulations of Mesoscale Topographic Effects', *Boundary-Layer Meteorol.* **49**, 169–195.

Huang, C. Y. and Raman, S.: 1990a, 'Numerical Simulations of Cold Air Advection over the Appalachian Mountains and the Gulf Stream', *Mon. Wea. Rev.* **118**, 343–362.

Huang, C. Y. and Raman, S.: 1990b, 'A Comparative Study of Advection Schemes with a Modified WKL Scheme', submitted to *Mon. Wea. Rev.*

Mellor, G. L. and Yamada, T.: 1974, 'A Hierarchy of Turbulence Closure Models for Planetary Boundary Layers', *J. Atmos. Sci.* **31**, 1791–1806.

Mellor, G. L. and Yamada, T.: 1982, 'Development of a Turbulence Closure Model for Geophysical Fluid Problems', *Rev. Geophys. Space Phys.* **20**, 851–875.

Moeng, C. H. and Wyngaard, J. C.: 1989, 'Evaluation of Turbulent Transport and Dissipation Closures in Second-Order Modeling', *J. Atmos. Sci.* **46**, 2311–2330.

Nicholls, S.: 1985, 'Aircraft Observations of the Ekman Layer during the Joint Air-Sea Interaction Experiment', *Q. J. R. Meteorol. Soc.* **111**, 391–426.

Redelsperger, J. L. and Sommeria, G.: 1986, 'Three-Dimensional Simulation of a Convective Storm: Sensitivity Studies on Subgrid Parameterization and Spatial Resolution', *J. Atmos. Sci.* **43**, 2619–2635.

Sun, W.-Y. and Ogura, Y.: 1980, 'Modeling the Evolution of the Convective Planetary Boundary Layer', *J. Atmos. Sci.* **37**, 1558–1572.

Yamada, T. and Mellor, G.: 1975, 'A Simulation of Wangara Atmospheric Boundary Layer Data', *J. Atmos. Sci.* **12**, 2309–2329.

Yamada, T.: 1983, 'Simulations of Nocturnal Drainage Flows by a q^2l Turbulence Closure Model', *J. Atmos. Sci.* **40**, 91–106.

Warming, R. F., Kutler, P. and Lomax, H.: 1973, 'Second- and Third-Order Noncentered Difference Schemes for Nonlinear Hyperbolic Equations', *AIAA J.* **11**, 189–196.

Wayland, R. and Raman, S.: 1989, 'Mean and Turbulent Structure of a Baroclinic Marine Boundary Layer during the 28 January 1986 Cold-Air Outbreak (GALE86)', *Boundary-Layer Meteorol.* **48**, 227–254.

Wyngaard, J. C., Coté, O. R. and Rao, K. S.: 1974, 'Modeling the Atmospheric Boundary Layer', *Adv. Geophys.* Vol. 18A, Academic Press, pp. 193–211.